PHYSICAL MODELING OF HYDRAULIC DESILTATION IN TAPU RESERVOIR

Jihn-Sung LAI[1] and Fi-John CHANG[2]

ABSTRACT

A movable bed physical model was constructed to investigate hydraulic desiltation by flushing and lateral erosion in the Tapu reservoir, Taiwan. The model scaling is based on the requirement for dynamic similarity of cohesive sediment deposit initiation in flushing processes. For model scaling, flume experiments investigating the initiation of cohesive sediment deposits were carried out to establish the relationship between critical shear stress of the flow and dry density of the deposit. Experiments in the physical model were then performed to measure the variations of the reservoir water level, the outlet discharge and the outflow sediment discharge. The processes of emptying and flushing were observed and analyzed in the main flushing channel. One of the experiments was conducted to simulate the on-site flushing operations on June 11, 1997. The results showed that the total cumulative flushed sediment volume by physical modeling was close to that by numerical simulation. To deal with the floodplain deposits, experiments of lateral erosion as an auxiliary method were also conducted in the physical model to investigate the effectiveness and applicability for the Tapu reservoir.

Key Words: Physical model, Hydraulic desiltation, Cohesive deposits, Emptying and flushing, Lateral erosion

1 INTRODUCTION

In recent years, the concept of long-term sustained use of reservoirs has been addressed because a reservoir is very much considered to be a nonrenewable resource (Morris and Fan, 1998). Technically, many options for reservoir sedimentation control can be utilized to pursue the sustainable development of water resources. In general, reduction of incoming sediment yields from watersheds is often employed in conjunction with hydraulic methods such as flushing or density current venting, but it requires long-term efforts to achieve the desired goal. Mechanical removal by dredging or dry excavation can regain the storage capacity immediately, but it is usually considered as the last measure due to its higher cost and disposal problems. Hydraulic methods have been applied successfully and found to be efficient and inexpensive in many cases (Shen and Lai, 1996; Zhang and Chien, 1985). In Taiwan, only few reservoirs have conducted desilting operations by hydraulic flushing due to lack of sediment release outlets in most of the reservoirs. The removal of sediment deposits by means of dredging or excavation is generally expensive, but it is frequently used because water is valuable for the strong demand of water supply in Taiwan (Hwang and Lai, 1996).

The Tapu reservoir with initial storage capacity of 9.26×10^6 m^3 was completed in 1960. According to a reservoir bed elevation survey in 1987, cumulative deposits once filled up 51.0% of the initial storage capacity due to intensive mining activities in its watershed and lack of proper measures for reservoir desiltation. Serious sedimentation has raised the flood stage along the tail reach of the reservoir, threatened the safety of local people, and forced the government to build levees for protection.

[1] Assistant Research Fellow, Hydrotech Research Institute, National Taiwan University, Taipei, 10617, Taiwan

[2] Professor, Department of Agriculture Engineering and Hydrotech Research Institute, National Taiwan University, Taipei, 10617, Taiwan

Note: The manuscript of this paper was received in Nov. 2000. The revised version was received in April 2001. Discussion open until Sept. 2002.

Fortunately, the Tapu reservoir has a sluiceway facility and gorge-shaped reservoir geometry. It has the potential to flush sediment through. With a 3.8 m × 8 m sluice gate, it has practiced several drawdown flushing operations by emptying the reservoir to remove a significant amount of deposits during typhoon or storm events since 1991. Furthermore, deposits in the Tapu reservoir contain a large portion of fine sediments and behave as cohesive materials (Chang and Lai, 1999).

A movable bed physical model of the Tapu reservoir was constructed to investigate hydraulic desiltation by flushing and by lateral erosion to deal with serious sedimentation problems. Theoretically, a physical model has to satisfy the similarity of geometric, kinematic and dynamic conditions and be capable of reproducing the flow and sediment behaviors in the prototype (Dou, 1998). There are commonly used parameters to represent the cohesive soil properties such as density, grain size, clay content, water content, temperature, etc (Raudkivi, 1998). According to previous research, however, physical models may not be able to scale cohesive sediment transport behaviors accurately (Morris and Fan, 1998).

Few researches have been reported on studying flushing processes in reservoirs with cohesive deposits by physical modeling. Wang and Zhang (1989) conducted experiments in a reservoir model scaled by using the relationship of critical velocity initiating cohesive sediment movement and dry density representing deposit erodibility. Accordingly, many researchers have found that the erosion potential with respect to bed shear strength of cohesive bed material can be related to the dry density of deposits (McNeil, Taylor and Lick, 1996; Mehta, et al. 1989). In the present study, flume experiments were performed to obtain the critical shear stress and velocity corresponding to the initiation of deposit erosion. A regressed relationship of critical shear stress (τ_c) and dry density (ρ_d) obtained and expressed simply as an exponential function was employed to establish the dynamic similarity of initiation of sediment movement. Although this relationship is very approximate and site-specific, it is useful for estimating the critical shear stress generated by water (or bed shear strength with respect to erosion) in the absence of a better correlation to properties characterizing deposit structure (Mehta, et al. 1989). Therefore, the model scaling by dynamic similarity of sediment initiation and erosion during flushing processes can be considered. Additionally, a consolidating bed causes the time-varying density of the bed deposits. The accompanying density increase with time changes the erodibility of the consolidating bed in bed shear strength. To estimate the time-varying erosion potential of consolidating bed deposit in the process of deposit paving in physical model, the dry density of bed deposit against time was also obtained through laboratory experiments.

To study hydraulic desiltation in the physical model, experiments were performed to measure water level variations in the reservoir, outlet discharges and outflow sediment discharges. During the processes of emptying and flushing, formation of flushing cone and flushing channel, and processes of retrogressive erosion and progressive erosion can be observed and analyzed. Meanwhile, experiments of lateral erosion as an auxiliary method on floodplain are also conducted in the physical model to investigate its effectiveness and applicability for the Tapu reservoir.

2 DESCRIPTION OF TAPU RESERVOIR

The Tapu reservoir has a natural drainage area of 100 km^2. It is formed by the Tapu dam located on the middle reach of the Aumei river and about 6 km from the junction with the Chungkung river which flows westward to the Taiwan Strait. The mean annual inflow is 1.76×10^8 m^3. The watershed area of the Tapu reservoir is presented in Fig. 1. Water supply and flood control are the main functions of the Tapu reservoir. The Tapu dam, which was constructed during the period of 1956 – 1960, is a 20.9 m high and 98.9 m long concrete gravity dam with four spillways (8.3 m high, 8 m long each) and one sluiceway (3.8 m high, 8 m long) controlled by tainter gates. As shown in Fig. 2, the elevations of the spillway crest and the sluiceway crest are 61.8 m and 55.5 m, respectively. The design capacity of the four spillways is 1,937 m^3 /s, and of sluiceway is 440 m^3 /s. With a maximum level of 69.6 m, the reservoir pool impounds about 8 km in length and forms a water surface area of 135 ha. The initial storage capacity was 9.26×10^6 m^3, and the active storage was 7.96×10^6 m^3. The geometry of the Tapu reservoir is of gorge shape except the lake-like area, which is between 300 m and 1,100 m away from the dam. A small island is located in the middle of the lake-like area and divides the flow into two streams. The

main stream runs on the left side of the island. Basic data of hydrology, topography, hydraulic structures, and sedimentation survey were collected for setting up the physical model.

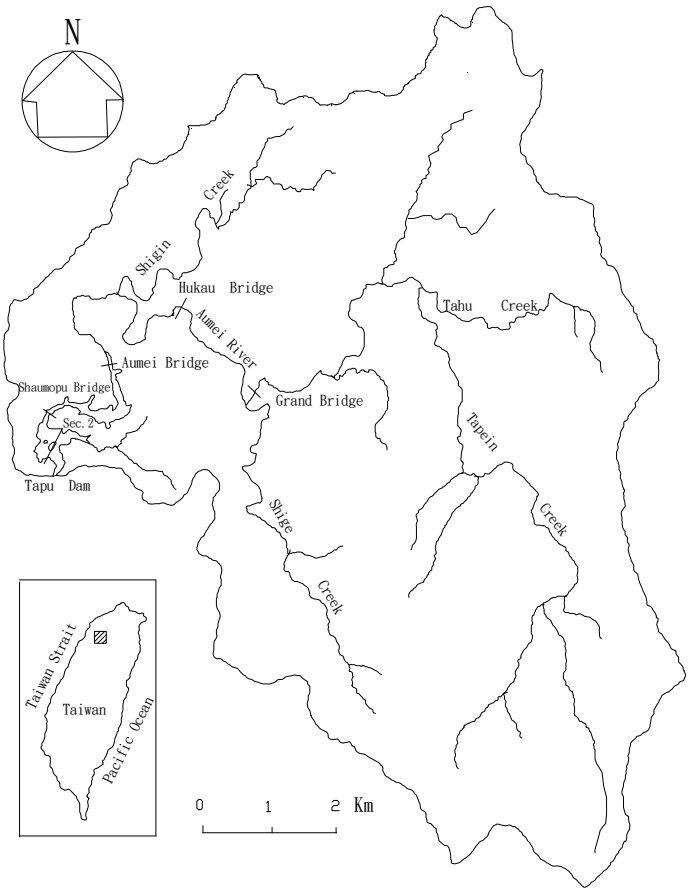

Fig. 1 Watershed area of Tapu Reservoir

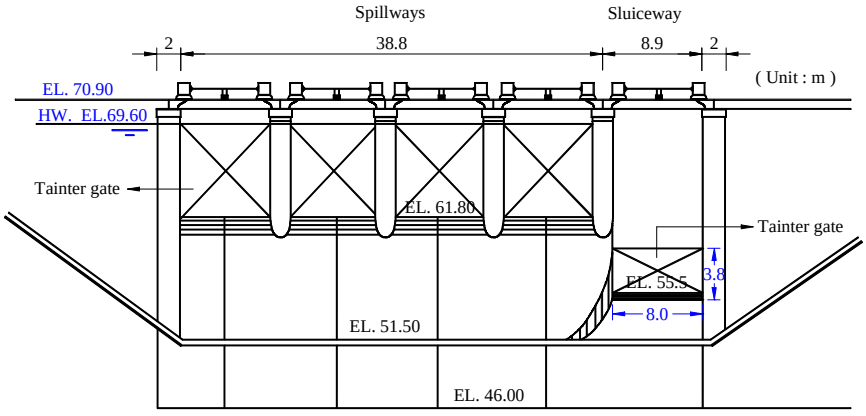

Fig. 2 Dam structure viewed from upstream side

2.1 Sedimentation

From the historical records of water levels at the Tapu dam, it was found that water level had been kept relatively high for water demand by obeying the original reservoir operational rule. For instance, the ten-day average water stages of the reservoir at the dam from 1987 to 1991 are plotted for each year in Fig. 3. Consequently, incoming sediment particles have settled down rapidly along the reservoir since the dam was completed. Based on the survey data, bed elevations of some cross sections measured along the reservoir are plotted in Figs. 4(a) through 4(d), which show that sediments mainly deposit on the main channel horizontally (Lai, 1998b). Corresponding to the water level and average bed elevation, the longitudinal bed profile along the reservoir is plotted in Fig. 5. As shown in Fig. 5, the Tapu reservoir has accumulated a significant amount of sediment after dam completion. The depositional pattern has become wedge-shaped since 1981 (Chang and Lai, 1999). Fig. 6 presents the reservoir storage capacity as well as active storage changes against time. The reservoir outflow discharges by ten-day period are also plotted in Fig. 6. There is no significant relationship between the discharge and the amount of cumulative deposits. However, intensive quartz-sand mining activities produced a great amount of sediment yield in the upstream watershed from 1961 to 1971. This also indicates that inflowing sediment had deposited significantly in the Tapu reservoir within the first ten years. As a result, the reservoir lost 43.3% of its initial storage capacity, and the estimated average yearly trap efficiency was about 83.3% before 1971. Although the depositional rate had slowed down, the storage capacity remained lost after 1971. According to a sedimentation survey in 1987, about 51.0% of the initial total storage capacity (or 43.3% of its initial active storage) had been filled up (Lai, 1998a). Due to desilting operations, the reservoir storage capacity was regained by flushing and dredging. By recent survey data in 1997, the storage capacity was regained, and it was estimated to be 59.4% of its initial storage capacity.

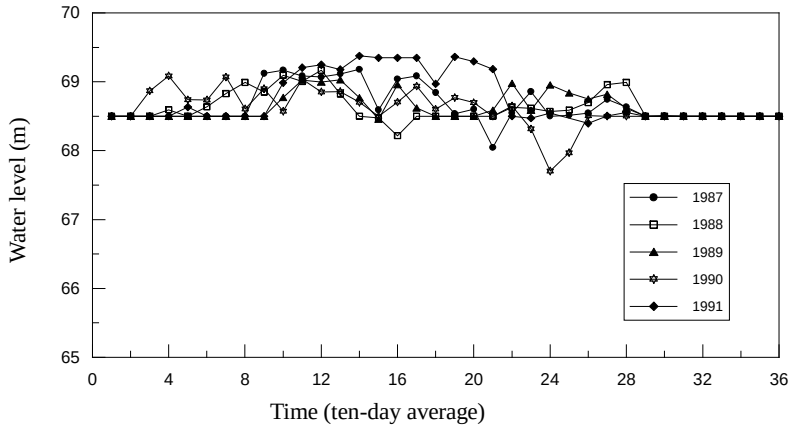

Fig. 3 Ten-day average water level records in Tapu reservoir from 1987 to 1991

2.2 Desilting Operations

In Taiwan, most of the reservoirs lack sediment release outlets, and only few reservoirs have conducted desilting operations by flushing. Fortunately, the Tapu reservoir has a sluiceway facility, and with a gorge-shaped reservoir geometry it has the potential to flush sediment. On the other hand, the Tapu reservoir has a small hydrologic size, that is, its initial storage capacity to mean annual inflow ratio (C/I = 9.26×10^{6} m^{3}/1.76×10^{8} m^{3}) is 0.053, which is far less than the empirical value 0.3 (Morris and Fan, 1998). This may imply that the Tapu reservoir can be refilled quickly when the flushing operation is terminated. According to water stage records, ten effective flushing operations were conducted with reservoir water level drawdown to restore reservoir storage capacity during 1991 to 1997. In those operations, reservoir water levels were fully drawn down to flush sediment through. However, there were no field measurements of sediment data in each flushing event.

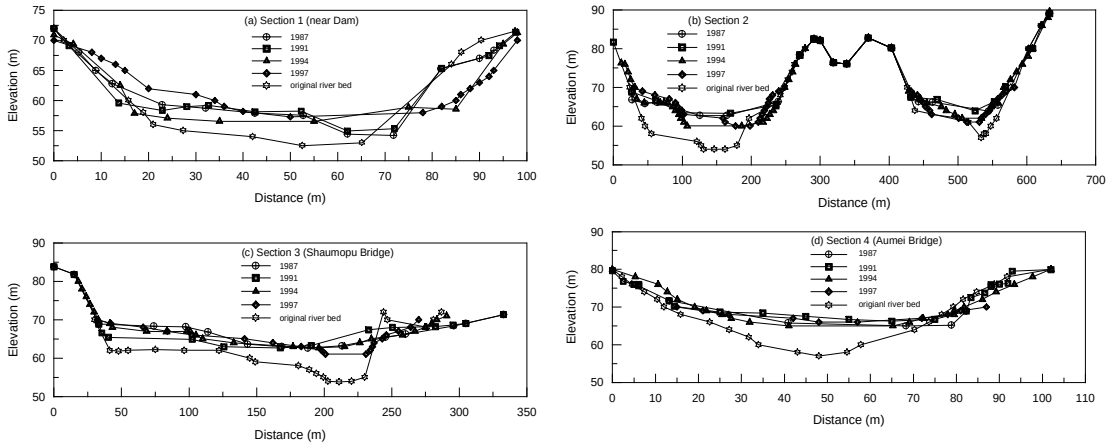

Fig. 4 Cross section variations along the Tapu reservoir

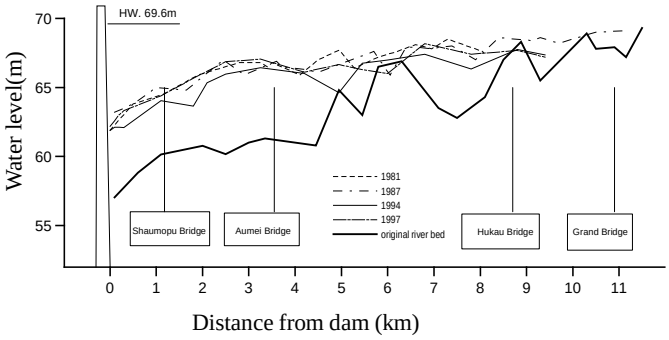

Fig. 5 Longitudinal bed profile variations along Tapu reservoir

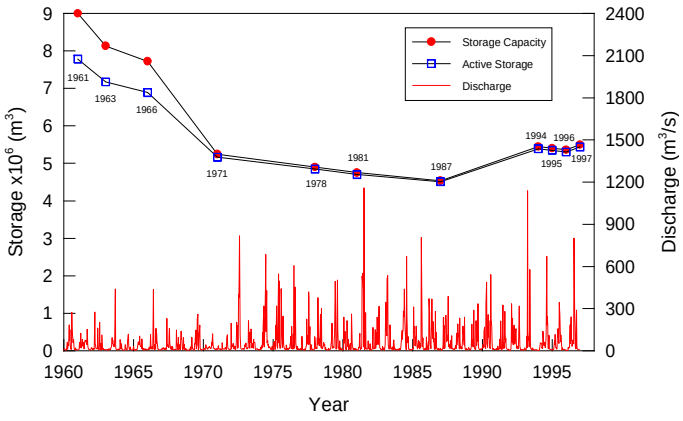

Fig. 6 Reservoir storage and outlet discharge changes by year

Because drought seasons occurred in 1993 and in 1996, there were two dry excavation operations to remove deposits in the Tapu reservoir, especially on the floodplain. Excavated zones are shaded and shown in Fig. 7. By means of dry excavation, mechanical removal using excavators was operated by removing and by trucking deposit materials in the period starting in late 1993 for 3 months. The excavated area shown in the zone A of Fig. 7 ranged from 550 m to 850 m away from dam. About 0.64×10^6 m^3 of deposits were removed. The other dry excavation operation in the Tapu reservoir was

conducted in the period starting in early 1996 for 2 months. The excavated zone B is shaded in Fig. 7. There were about 0.54×10^6 m^3 of deposits removed. The depth along the main stream was excavated down to the elevation of 60.4 m, and the elevation of the floodplain was lowered to 63.5 m. The average cost for dredging operation was about \$2.25 US/m^3 at that time. Based on the above data, the total amount of reservoir deposits removed by dry excavation was 1.18×10^6 m^3.

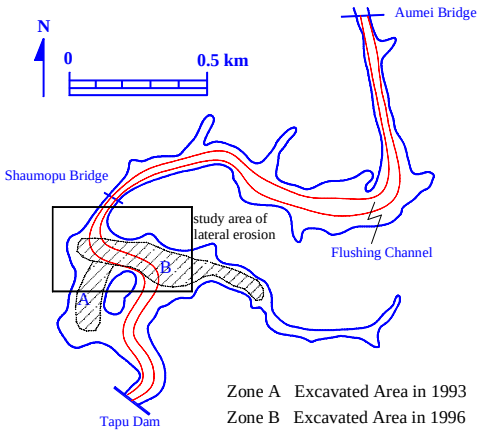

Fig. 7 Flushing channel and dry excavation areas

Referring to Fig. 6, the trend of storage capacity decreases quite linearly from 1971 to 1987. Without desilting operations, the storage capacity loss in the period of 1971 through 1987 was estimated to be 0.045×10^6 m^3/yr. Assume that incoming sediment yield from upstream was about the storage capacity loss per year after 1987. Therefore, the estimated amount of sediment deposits was 0.45×10^6 m^3, which had accumulated between 1987 and 1997. From sedimentation survey data in this period, the storage capacity had regained 1.07×10^6 m^3. Except for removal of floodplain deposits by dry excavation, there could have been 0.34×10^6 m^3 deposits removed mainly by flushing operations during 1991 through 1997. Nevertheless, sediment yield may be underestimated in each flushing operation because it usually happens in typhoon or storm event which can bring much more sediment from the upstream watershed than that estimated merely by the yearly data. Thus, the combination of flushing operation and excavation operation can be effective for removing sediment deposits not only in the main flushing channel but also on the floodplain.

2.3 Sediment Deposit with Cohesiveness

Undisturbed sediment samples were collected from reservoir deposits by a gravity corer. Grain size distributions of five samples are plotted in Fig. 8. Samples 1 through 4 were obtained from the disposal site, which were excavated from the locations near the dam in 1996, and Sample 5 was obtained directly from the location near the dam by gravity corer. About 65% of fine-grained sediments pass the No. 200 sieve. On average, the sediments contain clay of 29%, silt of 43% and sand of 28%. The mean diameter is 0.0175 mm. Therefore, the reservoir deposits contain large portions of the fine sediments and behave as cohesive materials.

As mentioned above, the property of sediment deposit with cohesiveness is entirely different from that of non-cohesive material. In flushing processes, the eroding potential of cohesive deposits can be related to the dry density of sediment deposits (Mehta, et al. 1989). To determine the parameter of dry density, several undisturbed sediment samples in the field were collected at various locations shown in Fig. 9(a). The samples were dried overnight in the oven to obtain the dry density of each sample. As shown in Fig. 9(b), dry density was plotted against distance away from the dam. The dry density of sediment deposit is lower if the sampling location is closer to the dam. The lower the dry density the softer sediment deposits, that is, the deposits with lower dry density tend to be eroded more easily.

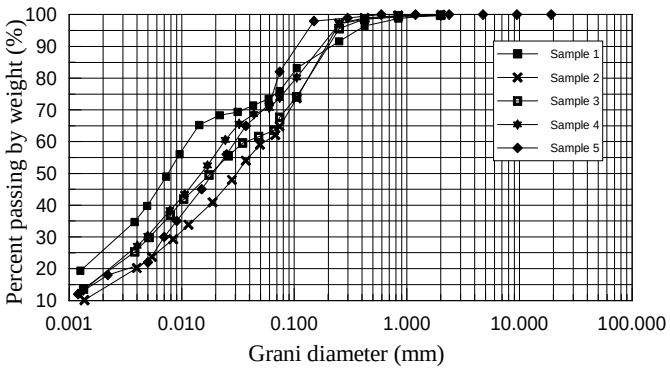

Fig. 8 Sediment size distribution near the dam

(a) Sampling Location

(b) Dry Density at Each Sampling Location

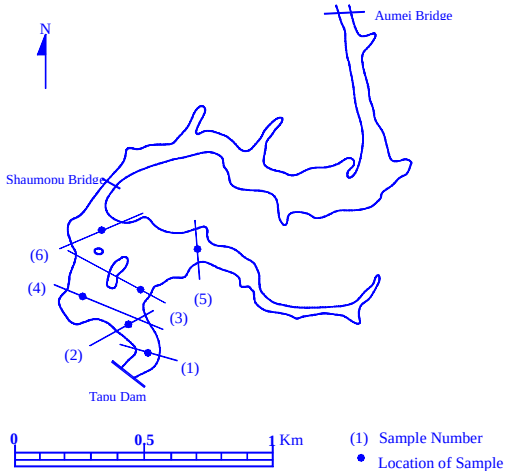

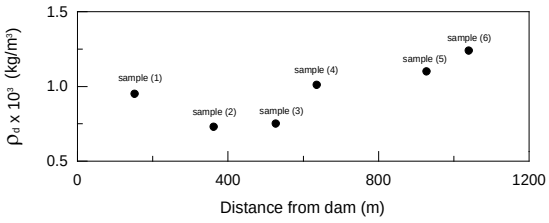

Fig. 9 Sampling location and dry density of deposit sample against distance

3 MODEL LAYOUT AND MODEL SCALING

3.1 Layout of Physical Model

Due to the limitation of the construction space, the geometric scale ratios of model to prototype were determined to be 1:100 in both vertical and horizontal directions. Thus, the physical model of the Tapu reservoir is an undistorted model with a geometry scale of $\lambda_L = \lambda_h = 1/100$. The subscripts L and h denote horizontal length dimension and vertical length dimension, respectively. The cross section selected at the upstream end as the inflow boundary should be relatively straight and uniform for water and sediment supply control purposes. The river reach near Section 13 located about 4 km away from the dam is relatively straight. In Fig. 4(d), the patterns of deposition and erosion at the cross section 13 (Aumei bridge) selected as the upstream control section are quite uniform in various years. In view of the cross section variations in Fig. 4, the shape of the cross section remains relatively unchanged to reveal the condition of equilibrium at the cross section 13. The downstream boundary is set at the cross section of the Tapu dam. The layout of the physical model is sketched in Fig. 10.

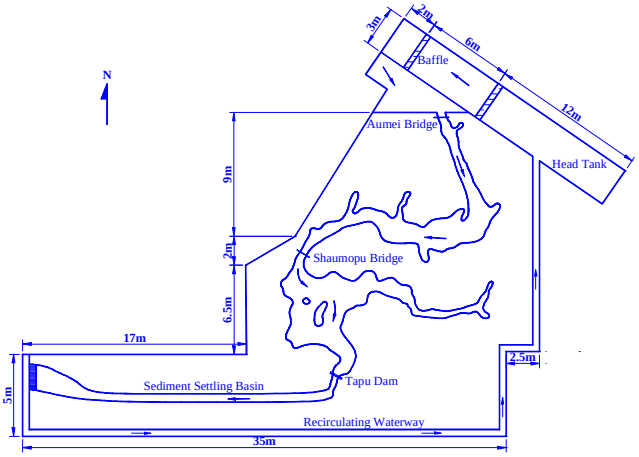

Fig. 10 Layout of the physical model

3.2 Similitude for Model Scaling

A physical model should be able to simulate closely the phenomena which take place in the prototype. Essentially, a physical model must satisfy the similarity of geometric, kinematic and dynamic conditions. In the open channel flow, most of the cases satisfying the dynamic condition by Froude number similarity are sufficient. According to the geometric scale constraints ($\lambda_L = \lambda_h = 1/100$); therefore, the flow velocity scale is $\lambda_u = \lambda_h^{1/2} = 1/10$, the flow discharge scale is $\lambda_Q = \lambda_u \lambda_A = \lambda_L^{5/2} = 1/10^5$, and the time scale is $\lambda_t = \lambda_L^{1/2} = 1/10$, in which λ is the ratio of model to prototype. The subscripts u , Q , A and t denote velocity dimension, discharge dimension, cross section area dimension and time dimension, respectively.

(a) Dynamic similarity of eroding processes during flushing

In order to achieve dynamic similarity in an alluvial system along with the Froude number similarity, parameters describing the sediment transport behaviors are usually adopted for model scaling. According to the flushing processes with strong tractive force acting on the surface of bed deposits, the fine sediment deposits with cohesiveness can be carried away as they are picked up by the flushing flow, and then may behave as wash load (Wang and Zhang, 1989).

Within a certain flushing reach (ΔL), the flushing flow generates bed shear force acting on the surface of sediment deposits to result in scouring depth (Δz), and over a time interval the entire amount of eroded deposit is $\rho_d V_S \left(= \rho_d B \Delta z \Delta L\right)$, where *B* is the width of the cross section in the flushing channel, ρ_d is the dry density, and V_S is the volume of the deposits eroded. At this moment, the average sediment concentration by weight at the cross section can be expressed as $S = \frac{1}{h}\int_0^h C(y)dy$, in which *C(y)* is concentration distribution along the vertical direction of the water column, and *h* is water depth. The total amount of eroded sediment in the water column is $SV\left(= SBh\Delta L\right)$. The amount of sediment deposit eroded from the bed approximately equals that suspended in the water column, that is, $SV = \rho_d V_S$. As the requirement of dynamic similarity during flushing, the sediment concentration ratio of model to prototype (λ_S) can be written as:

$$\lambda_S = \frac{\lambda_{\rho_d}\lambda_{V_S}}{\lambda_V} = \frac{\lambda_{\rho_d}\lambda_L^3}{\lambda_L^3} = \lambda_{\rho_d} \tag{1}$$

Equation (1) indicates the scale ratio of model to prototype for sediment concentration is equal to the scale ratio of dry density.

(b) Dynamic similarity of initiation of sediment movement

As mentioned previously, the erosion potential with respect to flow shear strength which can be related to the dry density of cohesive deposits by an exponential form, has been found by many researchers (Mehta, et al. 1989). Although this relationship is rather approximate and site-specific, it is useful for estimating the critical shear stress generated by flushing water in the absence of a better correlation to the properties characterizing the structures of reservoir deposits with cohesiveness. The regressed relationship of critical shear stress (τ_c) and dry density (ρ_d) can be written simply as $\tau_c = \alpha \rho_d^{\beta}$, in which coefficient α and exponent β can be obtained from flume experiments. In the open-channel flow, the logarithmic resistance law for rough boundaries is expressed as $u / u_* = f(R / k_s)$ (Garde and Ranga Raju, 1985), in which u is average velocity at cross section, u_* ($=\sqrt{\tau / \rho_w}$) is the shear velocity, R is hydraulic radius, k_s is equivalent roughness of sediment, and ρ_w is water density. Accordingly, the average velocity is proportional to the shear velocity. In the flushing reach, the shear velocity scale ratio (λ_{u_*}) may be assumed to be the average velocity scale ratio (λ_u). To initiate the movement of sediment deposits, the critical shear stress related to dry density of deposit is:

$$\tau_c = \rho_w u_{*c}^2 = \alpha \rho_d^{\beta} \tag{2}$$

in which u_{*c} is critical shear velocity. For model scaling based on the above expression and Froude number similarity of flow, the scale ratio of dry density (λ_{ρ_d}), therefore, can be expressed as:

$$\lambda_{\rho_d} = \lambda_{\tau_c}^{1/\beta} = \lambda_{u_{*c}}^{2/\beta} \cong \lambda_{u_c}^{2/\beta} = \lambda_h^{1/\beta} \tag{3}$$

in which u_c is critical velocity. According to Equations (1) and (3), the model scale ratio of sediment concentration resuspended in the water column is $\lambda_h^{1/\beta}$. The exponent β can be determined by flume experiment. The experiment setup and procedures will be described briefly in the next section.

(c) Bed deformation and time scaling

Bed variation during the flushing per unit width of the flushing channel can be described by sediment continuity equation:

$$\frac{\partial (qS)}{\partial x} + \rho_d \frac{\partial z_b}{\partial t'} = 0 \tag{4}$$

where q is the discharge per unit width, x is distance, z_b is bed elevation, and t' is time of bed variation. By model similarity, Equation (5) can be derived from Equation (4) and written as:

$$\frac{\lambda_q \lambda_S}{\lambda_x} = \lambda_{\rho_d} \frac{\lambda_{z_b}}{\lambda_{t'}} \tag{5}$$

in which $\lambda_x = \lambda_{z_b} = \lambda_L = \lambda_h$, $\lambda_q = \lambda_u \lambda_h = \lambda_h^{3/2}$ for undistorted model. Based on the relationships of Equations (1), (3) and (5), the time scale ratio of bed deformation due to eroding during flushing processes is $\lambda_{t'} = \lambda_L^{1/2} = 1/10$, and importantly it is the same as the time scale $(\lambda_t = \lambda_L^{1/2} = 1/10)$ of the flow part.

4 INITIATION OF SEDIMENT DEPOSITS

For further understanding of the critical shear stress acting on the bed to initiate the movement of the cohesive deposits, experiments were conducted in a 14 m long, 0.3 m wide and 0.6 m high tilting flume to

investigate the critical condition of deposit erosion in flushing processes. The sediment erosion can be observed through glass windows of the flume. Sediment deposit of desired dry density was paved in a box (15 cm long, 6 cm wide and 1 cm deep). The surface of the box with sediment deposit sample was carefully placed and leveled at the same elevation as that of the bed. Various discharges were supplied from the upstream to generate different shear stresses acting on the sample with desired dry density at temperatures ranging from 23 to 25 ^{o}C.

Compared with the non-cohesive deposits, the initiation of cohesive sediment movement is not easy to determine due to the difficulty in observing incipient motion on the bed surface. McNeil et al.(1996) described that sediment may not move for very low shear stresses. As the shear stress slowly increases, a few particles can be seen to roll along the surface. If the shear stress increases further, a small amount of erosion occurs as bursts of sediment at many small areas over the entire surface. The above descriptions of cohesive sediment erosion are qualitative; however, the critical condition of sediment initiation is still not clear defined. Based on the experimental measurements, a procedure was proposed by McNeil et al.(1996) to define the critical condition quantitatively. If more than 1 mm depth of sediment deposits is eroded at a certain shear stress in 2 minutes, the flow rate is decreased to give a new value of shear stress when erosion occurs, and at this moment the shear stress is defined as the critical shear stress. On the other hand, if less than 1 mm sediment deposit is eroded in 15 minutes, the flow rate is slightly increased to erode the deposits, and the shear stress under such flow condition is also defined as critical shear stress. Under this quantitative procedure, the critical shear stress causes an erosion rate between 10^{-3} and 10^{-4} cm/s. For the deposits sampled from the Tapu reservoir, the critical shear stress against dry density is calculated from the experimental results and plotted in Fig. 11. The corresponding critical velocities measured in the flume to initiate the bed deposits are also plotted together in Fig. 11. Regressed formulas for critical shear stress and critical velocity can be obtained:

As shown in Fig. 11, the critical shear stress as well as velocity can be related to the dry density by the exponential relationship, which provides a simple and quick estimation to correlate the flow characteristics with the cohesive deposit erodibility. Based on model scaling in Equations (1) and (3), one can have:

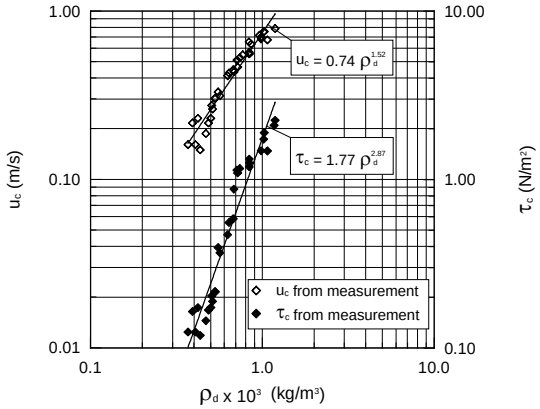

Fig. 11 Critical shear stress and critical velocity plotted against dry density

$$\tau_c = 1.77\ \rho_d{}^{2.87}; \qquad u_c = 0.74\rho_d^{1.52} \tag{6}$$

$$\lambda_S = \lambda_{\rho_d} = \lambda_{\tau_c}^{2/\beta} = \lambda_h^{1/\beta} = (1/100)^{1/2.87} = 1/4.98 \tag{7}$$

5 CONSIDERATION OF DENSITY VARIATION

Cohesive deposits form in processes of sediment settling and consolidation. In modeling deposit erosion, it is essential to consider the consolidation of a cohesive sediment bed due to the accompanying density changes of sediment mass eroded per unit bed thickness. In general, consolidating bed deposit

leads to continuing increase of critical bed shear strength with time. To estimate the time-varying erosion potential of consolidating bed deposit for sediment pavement in the physical model, the dry density changing with time is obtained by conducting laboratory experiments.

Dry deposits from Tapu reservoir were well mixed with water by the weight ratio of 1 to 3 at the temperature of about 25 ^{o}C. During the flushing event on June 11, 1997 after emptying in the Tapu reservoir, the field observation showed that the erosion depth was about 1 m – 3 m deep variously from Shaumopu to the dam. By sampling data from the field, the erosion depth of deposits mainly represented that close to the bed surface, and it was selected to be 2 cm deep (2 m deep in prototype) to consider the dry density of sediment deposits in the physical model.

As the experiment started, the 2 cm-inner diameter plastic tubing was inserted to catch 2 cm deep deposit from the mixture in a one-liter beaker at various times for each experiment. Data were collected at 2, 4, 6, 8, 10, 20, 30 minutes for each experiments, respectively. Each sample obtained was then dried overnight in the oven to calculate the dry density. Fig. 12 shows the experimental results of dry density varying with time.

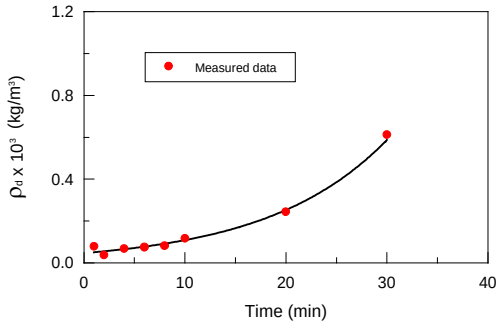

Fig. 12 Dry density varying with time

6 EXPERIMENTAL RESULTS AND ANALYSES

Beside dry excavation, flushing operations had been practiced several times in Tapu reservoir before 1997. By hydraulic desiltation, emptying and flushing with full reservoir drawdown was applied to flush sediment through. However, there were no data recorded from the field for inflow or outflow sediment discharge. In order to understand the flushing processes in the Tapu reservoir, experiments were performed to collect data in the physical model. During reservoir emptying, several flushing phenomena can be observed and analyzed such as formation of a flushing cone and flushing channel, and the processes of retrogressive erosion and progressive erosion. In the present study, three experiments (Run 1, Run 2 and Run 3) were conducted to analyze the characteristics of flushing processes. Before each run, the bed topography was templated and paved by the mixture of water and deposits excavated from field for desired dry density. The undisturbed samples collected in the field revealed that the average value of dry density was 960 kg/m^3. By the scale ratio of dry density, the desired dry density of model deposit was 193 kg/m^3. As found in Fig. 12, after 18 minutes the dry density of the sediment mixture paved in the model is about 193 kg/m^3 for starting to run the experiment. The procedures and results of each experiment will be described in Section 6.1.

On the other hand, based on the field and laboratory observations, the effective erosion areas are mainly along the flushing channel in the Tapu reservoir. Though sediment deposits can be removed in the flushing channel, floodplain deposits can not easily be removed without auxiliary methods such as by lateral erosion or by mechanical method. Except for mechanical methods, lateral erosion has been practiced quite successfully in China (Bureau of hydraulic and soil-water conservancy, 1989; Morris and Fan, 1998). It is designed by diverting river flow through a supply channel along the reservoir. In this study, experiments were conducted on a floodplain of the physical model to investigate the effectiveness and applicability of lateral erosion. The study area of lateral erosion was located at the zone B as shown in Fig. 7.

6.1 Reservoir Emptying and Flushing

Three cases of sediment removal by emptying and flushing were conducted in the physical model. Run 1 was set up with an initial water stage of 68.5m. There was no inflow imposed at the upstream to simulate the situation of an emptying operation. To start the experiment of Run 1, the sluice gate was fully opened within 30 minutes. In the time series, measurements of water levels were taken by the ultrasonic position sensors and point gages at the center of cross sections located near the sluice gate, at Shaumopu bridge, at Fushin bridge and at Aumei bridge. Also, outlet discharges were collected on the downstream side of the dam by time ranging from 50 to 80 seconds. The collected outflow sediment samples were dried overnight in the oven and weighed. The experimental results against time for Run 1 were transferred to the prototype and plotted in Fig. 13 for outlet discharge (Q_o), outflow sediment discharge (Q_s), and water levels. As shown in the figure, without inflow at the upstream the outlet discharge decreased rapidly as the water level dropped. At the early stage of flushing, the outflow sediment discharge was rather high soon after the sluice gate was opened. However, the outflow sediment discharge decreased dramatically until it ran about 100 minutes. Although bottom topography was invisible due to the high turbidity of flushing flow, in fact, high outflow sediment discharge should be caused by the formation of flushing cone under pressurized flow condition once described by several researchers (Di Silvio, 1990; Lai and Shen, 1996; Wang and Zhang, 1989). When the water level dropped approximately to the top of the sluice gate of level 59.3 m after 100 minutes, the pressurized flow condition near the sluice gate turned into open-channel flow condition to form a flushing channel mimicking the original river path (Basson and Rooseboom, 1996; Morris and Fan, 1998). At this moment, although the outlet discharge decreased significantly, the outflow sediment discharge increased because the water level near the sluice gate dropped to increase the overall water surface gradient in the reservoir. This was the phenomenon of retrogressive erosion observed in the physical model. After the peak of the outflow sediment discharge, erosion decreased quickly. Later, flushing ceased when water volume stored in the reservoir was completely drained.

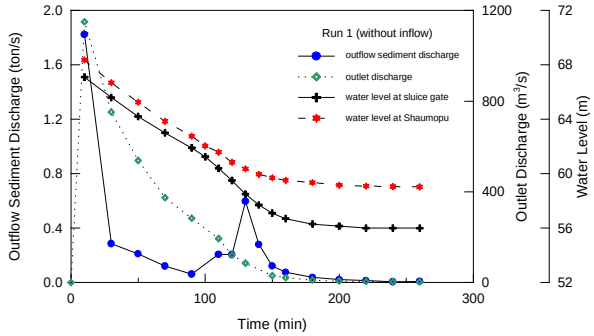

Fig. 13 Measurements of outflow sediment discharge, outlet discharge and water levels for Run 1

The outflow sediment discharge Q_s generated by flushing is useful for estimating the amount of flushed sediment, and it may be expressed as a function of the parameter such as $Q_o^{1.6} S_w^{1.2} / B^{0.6}$, in which Q_o is outlet discharge, S_w is water surface gradient in the flushing channel, and B is flushing channel width (Lai and Shen, 1995). Based on experimental results from Run1, each outflow sediment discharge obtained at each sampling time was plotted against the parameter in Fig. 14. The majority of data points fell on the regressive line except the data points circled with the dash line. It was found that these data points were obtained under pressurized flow condition at the early stage of flushing when the flushing cone adjacent to the sluice gate was formed.

For Run 2, the experiment was performed in two steps. In the first step, the procedures were the same as those of Run 1 until the reservoir was completely empty. Secondly, a constant discharge of 170 m^3/s — the capacity of the sluice gate, was supplied at the upstream boundary of the physical model to ensure that flow remained open-channel flow condition with sluice gate fully opened. This type of flushing

operation was to simulate the situation of emptying the reservoir before the flood season and waiting for a flood coming from the watershed. Fig. 15 shows the measured data of outlet discharge, outflow sediment discharge, and water level near the sluice gate. The outlet discharge increased as flushing flow reached the sluice gate, and the retrogressive erosion occurred to remove sediment deposits. However, after the retrogressive erosion ceased, the progressive erosion could only generate less concentration in outlet discharge.

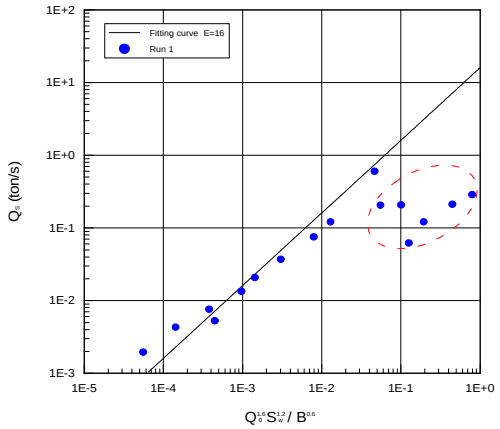

Fig. 14 Relationship between outflow sediment discharge and parameter $Q_o^{1.6} S_w^{1.2} / B^{0.6}$ for Run 1 in emptying and flushing operation

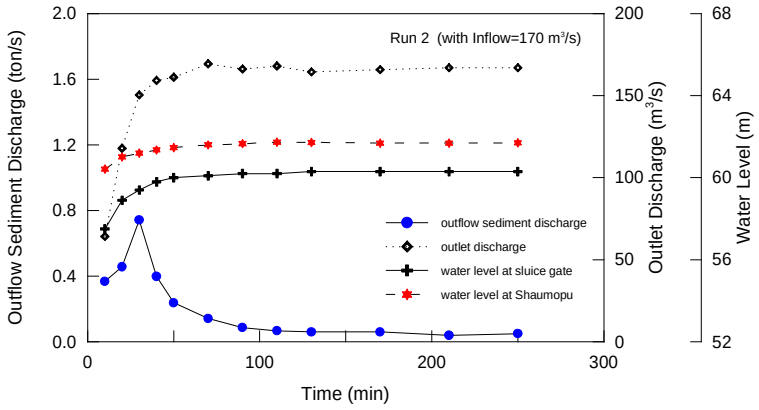

Fig. 15 Measurements of outflow sediment discharge, outlet discharge and water levels after the reservoir completely empty for Run 2

To simulate the flushing event on June 11, 1997 as Run 3, the procedures of gate operations in the physical model were exactly the same as those in the field. In Fig. 16, the outlet discharge and water level at the sluice gate were plotted and compared with field data. It showed that the physical model duplicated the flow condition in the field quite well. Without the field measurements for sediment, simulated results of cumulative flushed sediment volume by a numerical model based on the algorithm similar to that of HEC-6 model were plotted together in Fig. 17 with the data collected from the physical model.

Based on experimental data without those under pressurized flow conditions, outflow sediment discharge at each sampling time was also plotted against the parameter $Q_o^{1.6} S_w^{1.2} / B^{0.6}$ in Fig. 18 to show good correlation. The summary of experimental results is listed in Table 1.

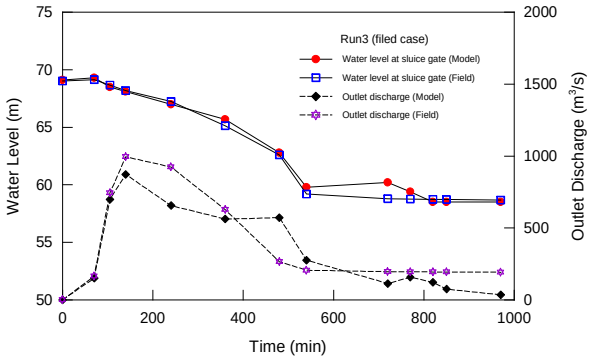

Fig. 16 Comparisons of water level and outlet discharge in model and in field

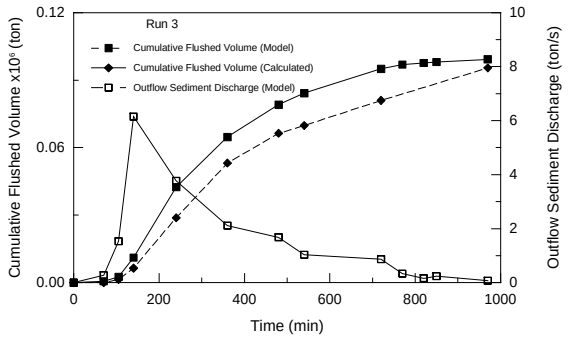

Fig. 17 Measured data comparing with numerical results of cumulative flushed volume for Run 3

Table 1 Experimental results of emptying and flushing operations (scaled by prototype)

Run No.	Running time (min)	Total flushed amount $\times 10^6$ (ton)	Average outflow concentration (kg/m^3)	Water/sediment (by volume)
1 (without inflow)	260	0.0035	2.48	2,950
2 (with inflow 170 m^3/s)	250	0.0021	0.27	27,090
3 (field case)	970	0.0943	3.98	1,840

6.2 Lateral Erosion on Floodplain

Experiments of lateral erosion were performed in zone B of this physical model as shown in Fig. 19. Basically, three parts of the facilities can be installed for operating lateral erosion, including water diverting system, supplying system and releasing turnout (Morris and Fan, 1998). By being released at desired points along the supply channel, the flow can generate corresponding side channels across floodplain deposits toward the main flushing channel. Lateral erosion can be performed only after the flushing channel has been created by drawdown operation or emptying the reservoir. It is found to be effective due to a significant bed slope gradient along side channel between flushing channel invert and supply channel turnout (Bureau of hydraulic and soil-water conservancy, 1989).

In Fig. 19, the supply channel may be built near the shoreline along the road which provides convenience for construction and maintenance. Based on the dry density (1,010 kg/m^3) obtained from the field around the excavated areas, three experiments were conducted in the physical model with constant flushing flow discharges of 0.41, 1.04 and 2.61 m^3/s. The experimental results included water surface slope in the side channel and outflow sediment discharge at each sampling time, and the average sediment concentration for each experiment. Similar to sediment discharge eroded in the flushing channel, lateral erosion rate (Q_{ls}) is useful for estimating the amount of eroded floodplain deposits and may be expressed as:

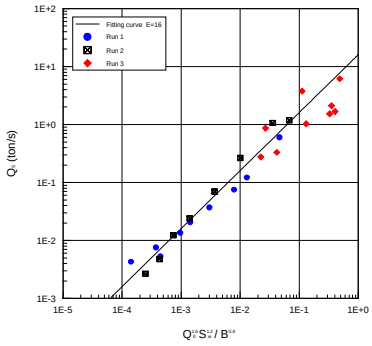

Fig. 18 Relationship between outflow sediment discharge and parameter $Q_o^{1.6} S_w^{1.2} / B^{0.6}$ for the three runs in emptying and flushing operation

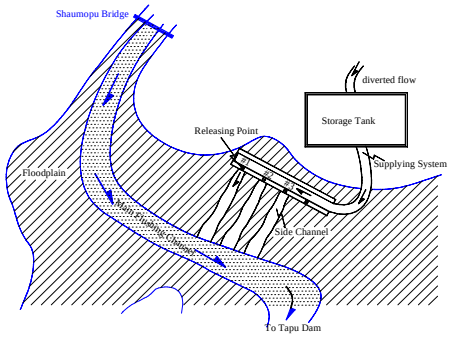

Fig. 19 Setup for experiments of lateral erosion

$$Q_{ls} = K\, Q_{lo}^{1.6}\, S_{lw}^{1.2} \tag{8}$$

in which K is erodibility coefficient, Q_{lo} is flushing flow discharge, and S_{lw} is water surface slope in the side channel. The site-specific K value is essentially related to the properties of floodplain deposits. Based on the relationship in Equation (8), data collected from the experiments were plotted in Fig. 20 and summarized in Table 2. With the other two sets of data from the Heisonglin reservoir and the Shiaodaokuo reservoir in Fig. 20, the experimental results seem to follow the tendency of Equation (8), and K is found to be 17.5 by regression (with R square 0.83). According to the field data from several reservoirs in China, the K values vary from 2.2 to 87.5 corresponding to various dry density. For instance, the average sediment concentration of Run 3 is 219 kg/m^3, and its ratio of water to sediment is about 32, which is similar to that recorded at the Shiaodaokuo reservoir in China (Bureau of hydraulic and soil-water conservancy, 1989).

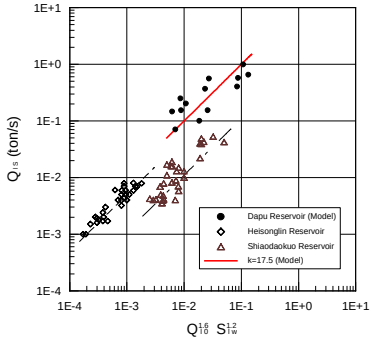

Fig. 20 Relationship between outflow sediment discharge and parameter $Q_{lo}^{1.6} S_{lw}^{1.2}$ in lateral erosion operation

Table 2 Experimental results for lateral erosion (scaled by prototype)

Run No.	Running time (min)	Flushing flow discharge (m^3/s)	Average sediment concentration (kg/m^3)	Water/sediment (by volume)
1	200	0.41	410	17
2	150	1.04	290	24
3	150	2.61	219	32

7 SUMMARY AND DISCUSSION

The undistorted movable bed physical model of the Tapu Reservoir was constructed to investigate hydraulic desiltation by flushing and lateral erosion for dealing with serious sedimentation problems. Regarding the sediment part, the model scaling is based on the requirement for dynamic similarity of cohesive sediment initiation during flushing. Flume experiments were carried out to obtain the relationship between the dry density of deposits and critical shear stress of initiation as well as to establish the scale ratio by satisfying the dynamic similarity of flushing processes. The flume experimental results were regressed and expressed as Equation (6). Based on Equation (6), the relationship between critical shear stress and critical velocity can be derived as:

$$\tau_c = 3.13 \ u_c^{1.89} \tag{9}$$

In the above, the value of the exponent of u_c is 1.89, which is close to 2, that is, it supports the assumption of the expression in Equation (3).

For efficient removal of sediment deposits in the reservoir, the combined operations of flushing and excavation were investigated. According to the flushing channel formation observed in the field and in the physical model, the desired excavation area in zone B does not need to include the part within the flushing channel as shown in Fig. 7. Therefore, the desilting operation by dry excavation in the Tapu reservoir should mainly focus on floodplain deposits. However, the disposal problems of excavated materials can not be solved easily, and additionally the drought season may not occur regularly in the future. Thus, lateral erosion practice on a floodplain seems an attractive alternative for removing sediment deposits in conjunction with emptying and flushing operation.

Experiments of emptying and flushing were performed to measure the variations of the water level in the physical model, the outlet discharge and the outflow sediment discharge. Run 1 and Run 2 were observed and analyzed. At the early stage of flushing, the high outflow sediment discharge was measured soon after the sluice gate was opened, and it should have been caused by the formation of the flushing cone. When the water level dropped close to the top of the sluice gate, the pressurized flow diminished and turned into open-channel flow to form a flushing channel mimicking the original river path. At that moment, even though the outlet discharge decreased significantly, the outflow sediment discharge increased due to the increase of overall water surface gradient in the reservoir. That was the phenomenon of retrogressive erosion observed in the physical model. Furthermore, the cumulative flushed sediment volume from the result of the field case (Run 3) was compared with that by numerical simulation to show reasonable predictions. Until the water level was fully drawn down in Run 3, the volume of flushed sediment deposits of 0.0943×10^6 m^3 was about 27.7% of the total estimated-flushed amount removed by flushing operations from 1991 through 1997. As listed in Table 1, the average concentration of outflow of Run 3 is 3.98 kg/m^3, and the ratio of water to sediment by volume for Run 3 is about 1,840.

Experiments of lateral erosion as an auxiliary method were also conducted in the physical model to investigate its applicability in the Tapu reservoir. Lateral erosion can be operated only after the flushing channel is created by flushing operation. With relatively little amount of water, lateral erosion is found to be effective due to a significant bed slope gradient along the side channel. From experimental results of lateral erosion presented in Table 2, the outflow sediment concentration is much higher than that of the flushing operation, although the flushing discharge is far less than that used in emptying and flushing operations. According to the summary listed in Table 2, the average ratio of water to sediment for those three runs of lateral erosion is 24, which is about 77 times less than that of the emptying and flushing

operation in the field case of Run 3. Obviously, this is attractive for removing sediment deposits on the floodplain in the Tapu reservoir.

Finally, more field data such as the bed topography before/after flushing, inflow/outflow water and sediment discharge during one flushing event are needed to calibrate the physical model for further applications.

REFERENCES

Basson, G. R. and Rooseboom, A. 1996, Flushing channel deformation during high flow drawdown flushing. Proc. of the International Reservoir Sedimentation Conference, Vol.2, Fort Collins, CO, USA, pp. 1107-1129.

Bureau of Hydraulic and Soil-Water Conservancy. 1989, Reservoir desiltation techniques, Water Resources and Electric Power Press, Beijing, China. (in Chinese)

Chang, F. J. and Lai, J. S. 1999, Investigation on reservoir sediment flushing and capacity preservation techniques with physical model study (III). Hydrotech Research Institute, National Taiwan University, Report No. 322. (in Chinese)

Chien, N. and Wan, Z. 1998, Mechanics of sediment transport, ASCE Press.

Di Silvio, G. 1990, Modeling desiltation of reservoir by bottom-outlet flushing. In: Shen H.W. (editor), Movable Bed Physical Models, Kluwer Academic Publ., Netherlands, pp. 159-171.

Dou, G. 1998, Development of physical model studies on sediment transport in China. 7th International Symposium on River Sedimentation, Hong Kong, Dec., pp. 649-660.

Garde, R.J. and Ranga Raju, K.G. 1985, Mechanics of sediment transportation and alluvial stream problems, 2nd Edition, Wiley Eastern Limited.

Hwang, J. S. and Lai, J. S. 1996, Sedimentation problems in PWCB reservoirs in Taiwan. International Conference on Reservoir Sedimentation, Vol. 3, Fort Collins, CO, USA, pp. 1475-1482.

Lai, J. S. and Shen, H. W. 1995, An experiment study on reservoir drawdown flushing, Intl. Jour. of Sediment Research, International Research and Training Center on Erosion and Sedimentation (IRTCES), Vol. 10, No. 3, 1995, pp. 19-37.

Lai, J. S. and Shen, H. W. 1996, Flushing sediment through reservoirs. Jour. of Hydraulic Research, Vol.34, No. 2, pp. 237-255.

Lai, J. S. 1998a, Sediment deposition and desilting operation in Tapu reservoir. 3rd International Conference on Hydro-Science and Engineering, Aug., Cottbus/Berlin, Germany.

Lai, J. S. 1998b, Physical modeling of reservoir sediment flushing, 7th International Symposium on River Sedimentation, Hong Kong, Dec., pp. 693-698.

McNeil, J., Taylor, C. and Lick, W. 1996, Measurements of erosion of undisturbed bottom sediments with depth, Jour. of Hydraulics Engineering, ASCE, Vol.122, No.6, pp. 316-324.

Mehta, A. J., McAnally, W. H., Hayter, E. J., Teeter, A. M., Schoellhamer, D., Heltzel, S. B. and Carey, W. P. 1989, Cohesive sediment transport, I: process description. Jour. of Hydraulic Engineering, ASCE, Vol. 115, No. 8, Aug., pp. 1076-1093.

Morris, G. L. and Fan, J. 1998, Reservoir sedimentation handbook, McGraw-Hill, Inc.

Raudkivi, A.J. 1998, Loose boundary hydraulics, Balkema, Rotterdam.

Shen, H. W. and Lai, J. S. 1996, Sustain reservoir useful life by flushing sediment. Intl. Jour. of Sediment Research, International Research and Training Center on Erosion and Sedimentation (IRTCES), Vol. 11, No. 3, Dec. 1996, pp. 10-17.

Wang, Z. and Zhang, S. 1989, Model study on emptying flushing in a reservoir with cohesive deposits. Jour. of Sediment Research, Vol.2, pp. 62-68 (in Chinese).

Zhang, R., and Chien, N. 1985, Reservoir sedimentation, in Chap. 1 of the Lecture Notes of the Training Course on Reservoir Sedimentation, Series of Publ. IRTCES, Beijing, China.